

## MIGRATION OF EXSOLVED CO<sub>2</sub> FOLLOWING DEPRESSURIZATION OF SATURATED BRINES

Ronald W. Falta<sup>1</sup>, Lin Zuo<sup>2</sup> and Sally M. Benson<sup>2</sup>

<sup>1</sup>Department of Environmental Engineering and Earth Sciences, Clemson University, Clemson, SC,  
29634, USA

<sup>2</sup>Department of Energy Resource Engineering, Stanford University, CA 94305, USA

Email: faltar@clemson.edu

### **ABSTRACT**

Geologic disposal of supercritical carbon dioxide in saline aquifers and depleted oil and gas fields will cause large volumes of brine to become saturated with dissolved CO<sub>2</sub> at concentrations of 50 g/L or more. As CO<sub>2</sub> dissolves in brine, the brine density increases slightly. This property favors the long-term storage security of the CO<sub>2</sub>, because the denser brine is less likely to move upwards towards shallower depths. While dissolved-phase CO<sub>2</sub> poses less of a threat to the security of shallower drinking water supplies, the risk is not zero. There are plausible mechanisms by which the CO<sub>2</sub>-laden brine could be transported to a shallower depth, where the CO<sub>2</sub> would come out of solution (exsolve), forming a mobile CO<sub>2</sub> gas phase.

Recent laboratory experiments of the exsolution process show that the exsolved gas-phase relative permeability is much lower than relative permeabilities measured during CO<sub>2</sub> core floods. Numerical simulations of upward brine migration through an open fault were performed using TOUGH2-ECO2N with the two types of relative permeability functions. When traditional coreflood relative permeabilities are used, upward flow of a CO<sub>2</sub> saturated brine leads to exsolution and the development of a highly mobile CO<sub>2</sub> gas phase. When exsolution relative permeabilities are used, the tendency for the exsolved CO<sub>2</sub> to migrate as a separate phase is greatly reduced, though not eliminated.

### **INTRODUCTION**

Reduction of greenhouse gas emissions to levels required to stabilize the global climate will require an unprecedented societal effort. It is widely agreed that multiple methods will be

needed to achieve these emissions reductions. The Intergovernmental Panel on Climate Change (IPCC) has identified carbon dioxide capture and storage (CCS) as one of several key approaches that could substantially contribute to greenhouse gas emissions reductions. CCS focuses on reducing the CO<sub>2</sub> emissions from large stationary sources, typically fossil-fueled electrical power plants. Several methods of CO<sub>2</sub> storage have been proposed, including deep ocean storage, mineral carbonation, and geologic sequestration. Of these three methods, geologic sequestration appears to be the most practical option, and there do not appear to be any insurmountable technical barriers to its widespread adoption (Benson and Cook et al., 2005).

Each of the CCS technologies will have three main components. First, the CO<sub>2</sub> must be separated from other gases (primarily nitrogen) in the combustion gas waste stream. This is currently done using a solvent extraction process, but other methods may become feasible in the future. The low-pressure CO<sub>2</sub> gas from the separation process is then usually compressed into a liquid or supercritical fluid for subsequent transport to a storage site. With geological sequestration, the captured CO<sub>2</sub> is injected into a specific geologic formation with the expectation that it will remain there for thousands of years and longer. Recent estimates of the storage capacity for geologic sequestration in the U.S. are on the order of several hundred times the current U.S. annual CO<sub>2</sub> emissions (NETL, 2007). Most of this capacity exists as deep saline (brine) formations.

## CO<sub>2</sub> PROPERTIES

CO<sub>2</sub> has several unique properties that must be considered in the design of a geologic storage project. Key among these are its low critical pressure and temperature. CO<sub>2</sub> becomes a supercritical fluid at a pressure of 73.82 bar and a temperature of 31.04°C. Below this pressure and temperature, CO<sub>2</sub> exists as a gas, liquid, or solid, depending on pressure and temperature. At normal atmospheric temperatures and pressures, CO<sub>2</sub> is always found as a gas, and its density can be calculated from the ideal gas law. For example, at room temperature, pure CO<sub>2</sub> gas has a density of 1.8 g/L. This is about 1.5 times the density of air.

As CO<sub>2</sub> gas is compressed, its density increases almost linearly, following roughly ideal gas behavior. However, as the critical pressure is approached, the gas becomes much more compressible, and density rapidly increases with increasing pressure. At this point, CO<sub>2</sub> gas is nearly 4 times more compressible than an ideal gas, and it is several times more compressible than other common gases such as methane, nitrogen, or oxygen. As the critical pressure is exceeded, the supercritical CO<sub>2</sub> phase density continues to rapidly increase until a pressure of roughly 90 bar is reached. Beyond this pressure, the increase in CO<sub>2</sub>-phase density is moderate.

Current strategies for geologic storage take advantage of the high density (and low viscosity) of supercritical CO<sub>2</sub>, injecting the CO<sub>2</sub> at depths where the hydrostatic pressure is somewhat above the critical pressure (Figure 1). Depending on the subsurface temperature, the depth where high CO<sub>2</sub>-phase density is achieved is around 800–900 m (~2600–2950 ft). Beyond this depth, little is gained in terms of storage efficiency, although storage security may increase.

The CO<sub>2</sub>-phase density at typical target injection depths ranges from about 600 to 800 g/L. While this represents a roughly 400-fold increase in density over atmospheric pressure conditions, the phase density is still much lower than that of water or brine. This causes a strong upward buoyancy force that can allow the supercritical (or gas phase) CO<sub>2</sub> to move upward towards the ground surface. This type of uncontrolled

vertical migration of a pure CO<sub>2</sub> phase has been the subject of numerous studies (Bachu et al., 1994; Pruess and Garcia, 2002; Pruess, 2005b; Doughty, 2007; Nordbotten et al., 2008). Most strategies for the injection of supercritical CO<sub>2</sub> require a cap rock or stratigraphic trap to prevent the vertical movement. Similarly, most CO<sub>2</sub> escape routes from storage formations consist of defects or penetrations in the confining layer.

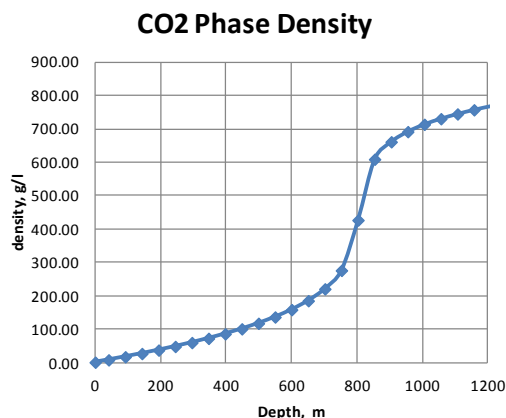


Figure 1. Variation in CO<sub>2</sub> density with depth at a temperature of 35°C (calculated using the TOUGH2-ECO2N equation of state package (Pruess, 2005a)).

Another important property of CO<sub>2</sub> is its high solubility in water and brines, especially at high pressure and low-to-moderate temperature. Starting at atmospheric pressure and 35°C, pure CO<sub>2</sub> gas has an aqueous solubility of about 1 g/l in a brine containing 10,000 mg/l NaCl. As the CO<sub>2</sub> pressure increases, the solubility rises nearly linearly, following Henry's Law (Figure 2). As supercritical pressure is approached, the rate of solubility increase flattens, and the solubility becomes a much weaker function of increasing pressure. At typical injection depths greater than 800 m (~2600 ft), CO<sub>2</sub> solubility can exceed 50 g/l, depending on the salinity and temperature.

The high solubility of CO<sub>2</sub> is significant in terms of geologic trapping. Consider a storage formation that is 900 m (2950 ft) deep in a formation at 35°C with salinity of 10,000 PPM. Under these conditions, the supercritical CO<sub>2</sub>-phase density is around 670 g/L, and the solubility in the brine is about 52 g/L. When the CO<sub>2</sub> phase occupies 7% of the pore space, an

equal mass of CO<sub>2</sub> is present in the formation dissolved in the pore water.

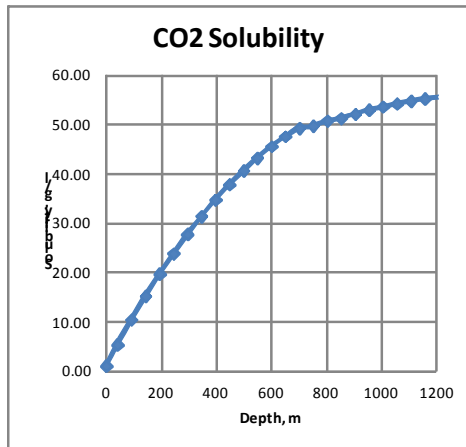


Figure 2. Variation in CO<sub>2</sub> solubility in a 10,000 mg/l NaCl brine at 35°C (calculated using the TOUGH2-ECO2N EOS)

As CO<sub>2</sub> dissolves in water or brine, the aqueous-phase density increases slightly. Over a pressure range from 1 to 155 bar at 35°C, a 10,000 mg/L brine will increase in density from about 1001 g/L to about 1006 g/L due to compression. If CO<sub>2</sub> is dissolved in the brine to its maximum solubility, the density increases with increasing depth. At hydrostatic pressures greater than roughly 60 bar (about 600 m or 2000 ft), the brine containing dissolved CO<sub>2</sub> is around 1% denser than the resident brine. This is a substantial contrast, and it is capable of driving buoyancy flows downward in the aqueous phase. The resulting natural convection flow is of significant interest because it tends to move the dissolved CO<sub>2</sub> down and away from the injected CO<sub>2</sub> phase (Ennis-King and Paterson, 2005; Farajzadeh et al., 2007; Hassanzadeh et al., 2007; Lindberg and Wessel-Berg, 1997). In general, this dissolved-phase CO<sub>2</sub> is believed to be more securely stored than separate-phase CO<sub>2</sub> due to the elimination of the upward buoyancy forces (Benson and Cook et al., 2005, Leonenko and Keith, 2008).

### CO<sub>2</sub> EXSOLUTION

The higher security of dissolved CO<sub>2</sub> compared to supercritical CO<sub>2</sub> has led some researchers to propose alternative injection schemes. For example, Leonenko and Keith (2008) and Burton and Bryant (2007, 2008) make a compelling case for injecting the CO<sub>2</sub> dissolved

in brine to prevent unwanted buoyancy flows of separate-phase CO<sub>2</sub>. Their feasibility studies suggest that dissolved CO<sub>2</sub> injection could compete with supercritical injection, although the capital and operating costs are somewhat higher due to the larger number of injection wells required. Leonenko and Keith (2008) also propose a promising alternative scheme in which a short period of CO<sub>2</sub> injection is followed by a long period of brine injection, to maximize the dissolution process.

Whether by design, or as a consequence of natural processes, it is clear that a significant fraction of the CO<sub>2</sub> that is geologically stored will eventually exist as a dissolved phase in the reservoir brine. While dissolved CO<sub>2</sub> presents a much lower release risk compared to free phase CO<sub>2</sub>, the risk is not zero. If a CO<sub>2</sub>-saturated brine is depressurized, the CO<sub>2</sub> will come out of solution (exsolve) and become a separate phase. The exsolved CO<sub>2</sub> is then free to migrate subject to large upward buoyancy forces. Consequently, CO<sub>2</sub> could move towards the ground surface and potentially contaminate shallower drinking waters supplies, as well as causing health, safety, and environmental hazards.

The most likely scenario for CO<sub>2</sub> exsolution from brine occurs when the CO<sub>2</sub>-saturated brine is transported towards the ground surface. Assuming that some type of high permeability pathway exists (such as a fault or abandoned well), only a moderate upward gradient is needed to mobilize brine. This upward gradient might be caused by groundwater pumping from an overlying aquifer, by high injection pressures in the storage formation, or it could exist naturally.

The necessary gradient for upward mobilization of a CO<sub>2</sub>-saturated brine can be calculated from Darcy's law. Following *Falta et al. [1989]*, the buoyancy velocity of a fluid of density  $\bar{\rho}$  through an ambient fluid of density  $\rho_{\infty}$  is:

$$V = -\frac{k}{\mu}(\bar{\rho} - \rho_{\infty})g \quad (1)$$

where  $k$  is the intrinsic permeability,  $\mu$  is the fluid dynamic viscosity, and  $g$  is the magnitude

of gravitational acceleration. The standard form of Darcy's law for a fluid of uniform density is

$$V = -K \frac{\partial h}{\partial z} \quad (2)$$

where  $K$  is the hydraulic conductivity,  $h$  is the hydraulic head, and  $z$  is elevation. The hydraulic conductivity is a function of both the porous media and fluid properties:

$$K = \frac{k \rho_{\infty} g}{\mu} \quad (3)$$

Substituting Equation (3) into (2), and equating the two forms of Darcy's law, the critical upward hydraulic gradient for mobilizing a dense fluid is:

$$\left| \frac{\partial h}{\partial z} \right| = \frac{(\bar{\rho} - \rho_{\infty})}{\rho_{\infty}} \quad (4)$$

Recalling that the brine density increase due to dissolved  $\text{CO}_2$  is around 1%, Equation (4) indicates that any upward gradient greater than 1% would be capable of mobilizing the  $\text{CO}_2$  saturated brine in the upward direction.

### RELATIVE PERMEABILITIES

Two-phase  $\text{CO}_2$ /water relative permeabilities are normally measured by flooding a core with the two fluids. Figure 3 shows a typical set of relative permeability primary drainage data measured by core flooding a Mount Simon sandstone [Zuo et al., 2012]. In this test, the  $\text{CO}_2$  phase was mobile at a saturation of 3% or less, and the relative permeability increases to a value of 0.38 at a  $\text{CO}_2$  saturation of 33%.

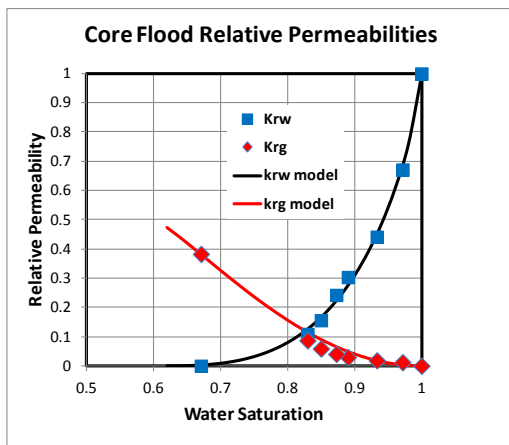


Figure 3. Relative permeabilities for a  $\text{CO}_2$ /water system measured during a core flooding experiment [Zuo et al., 2012]. The solid lines are best fits with Equations (5) and (6).

Zuo et al. (2012) performed exsolution experiments on cores that were initially filled with water saturated in dissolved  $\text{CO}_2$ . These experiments observed the evolution of the exsolved  $\text{CO}_2$  phase as the core confining pressure was dropped from 124.1 bar to 27.6 bar. During this depressurization, the  $\text{CO}_2$ -phase saturation increased from zero to a maximum value of about 40%. Mobilization of the  $\text{CO}_2$  phase occurred between 11.7 and 15.5% saturation, but the measured  $\text{CO}_2$ -phase relative permeability is extremely low. Figures 4 and 5 show a set of relative permeability curves measured on a Mount Simon sandstone using methods similar to those described by Zuo et al. (2012).

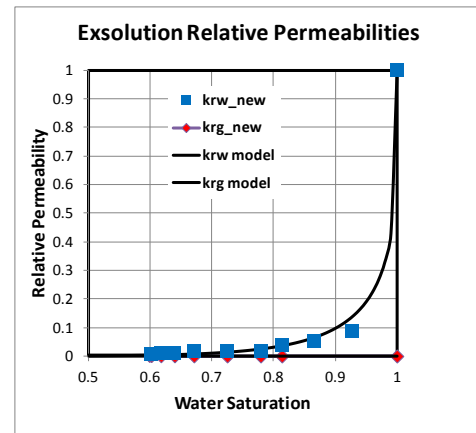


Figure 4. Relative permeabilities for a  $\text{CO}_2$ /water system measured during exsolution. The solid lines are best fits with Equations (5) and (6).

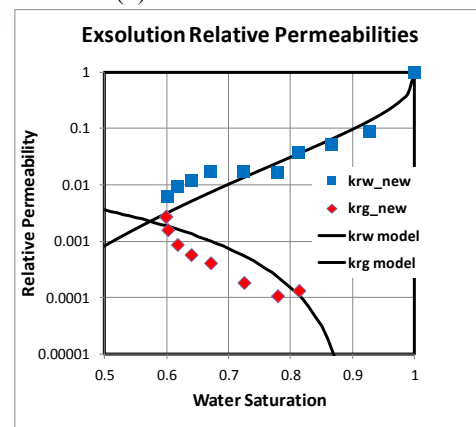


Figure 5. Relative permeabilities for a  $\text{CO}_2$ /water system measured during exsolution (log scale).

The exsolution relative-permeability values for the CO<sub>2</sub> phase are extremely low (Figure 5), with a maximum measured value of 0.003 at a CO<sub>2</sub> saturation of 40%.

## NUMERICAL SIMULATIONS

A series of simplified 2-D multiphase flow numerical simulations were performed to illustrate how a CO<sub>2</sub>-saturated brine could escape and result in uncontrolled vertical CO<sub>2</sub> migration to a shallow aquifer. These simulations were performed using the TOUGH2-ECO2N simulator (Pruess, 2005a; Pruess and Spycher, 2007). The scenario consists of a site with a surface elevation of 200 m above mean sea level (MSL). A 100 m thick saline aquifer is located at a depth of 900 m (an elevation of 700 m MSL). This aquifer has a salinity of 10,000 mg/l [L?] NaCl, and a temperature of 35°C. The formation has a vertical permeability of 10<sup>-12</sup> m<sup>2</sup> (a conductivity of 10<sup>-3</sup> cm/s), a horizontal permeability of 10<sup>-11</sup> m<sup>2</sup> and it is confined by a low permeability formation 600 m thick. A freshwater aquifer with the same permeability extends from a depth of 200 m to a depth of 300 m (elevations of 0 to -100 m MSL). The freshwater aquifer is hydraulically connected to the saltwater aquifer by a permeable fault zone (k= 10<sup>-11</sup> m<sup>2</sup>) that is 50 m wide (Figure 6). The brine aquifer is assumed to contain 50.7 g/l [L?] of dissolved CO<sub>2</sub>, which is just below the CO<sub>2</sub> solubility under these conditions. The saline aquifer is assumed to be large in extent and is maintained at a constant (hydrostatic) pressure over time.

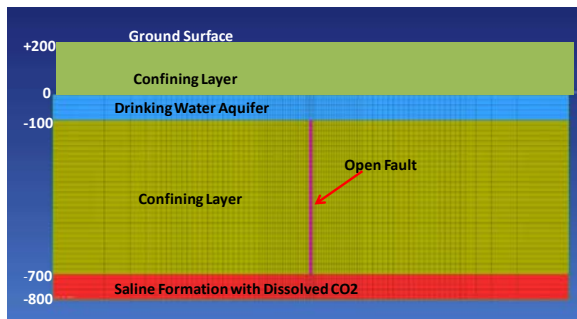


Figure 6. 2D cross sectional model of a saline formation containing dissolved CO<sub>2</sub> that is connected to a confined fresh drinking water aquifer by a high permeability fault zone

The relative permeability data in Figures 3 and 4 were fit using a modified version of the van Genuchten-Mualem model [Mualem, 1976; van Genuchten, 1980; Charbeneau, 2007]:

$$k_{rw} = \sqrt{S_w^*} \left\{ 1 - \left( 1 - S_w^{*/m} \right)^m \right\}^2 \quad (5)$$

and

$$k_{rg} = k_{rg\max} \sqrt{1 - \hat{S}_w} \left( 1 - \hat{S}_w^{1/m} \right)^{2m} \quad (6)$$

where

$$S_w^* = \frac{S_w - S_{wr}}{1 - S_{wr}}$$

and

$$\hat{S}_w = \frac{S_w - S_{wr}}{1 - S_{wr} - S_{gr}}$$

The factor  $k_{rg\max}$  is a scaling factor needed to match the relative permeability data. The model fits to the data are shown in Figures 3–5.

The system is initially in static equilibrium with a water table near the ground surface, and the CO<sub>2</sub> remains confined indefinitely in the deeper brine aquifer despite the presence of the open fault connecting the two aquifers. The hydrogeologic system is then perturbed by simulating groundwater pumping from the top of the confined fresh water aquifer. The hydraulic head at the top outer edges of the aquifer is reduced by 30 m (100 ft). This magnitude of hydraulic head decline is commonly observed in confined aquifers that are pumped for water supply or irrigation.

The drop in head in the aquifer is sufficient to mobilize the CO<sub>2</sub>-saturated brine upward through the fault zone, and into the freshwater aquifer. Figure 7 shows the CO<sub>2</sub> gas-phase saturations 30 years after the freshwater aquifer has been depressurized. Here, the CO<sub>2</sub>-laden saltwater is pulled upward through the fault and into the freshwater aquifer by the upward hydraulic gradient that was created by pumping the upper aquifer. As the brine moves up the fault, the pressure is lower, and the dissolved CO<sub>2</sub> partial pressure begins to exceed the water pressure. At this point, the CO<sub>2</sub> starts to exsolve, forming a separate gas phase. This simulation used the core-flood relative permeability

function (Figure 3). As the CO<sub>2</sub> comes out of solution, the evolving gas phase becomes mobile as its volumetric saturation increases. The mobility tends to further increase as the gas moves upward because of the large degree of expansion that occurs with depressurization (Figure 1).

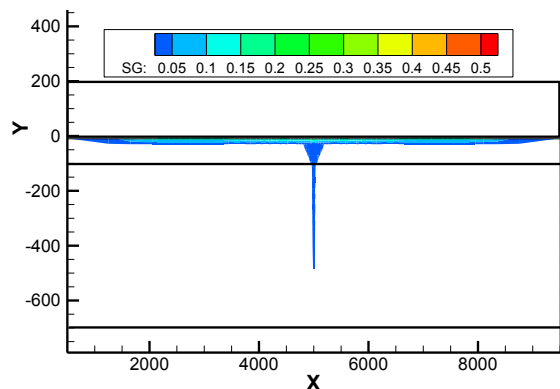


Figure 7. Simulated CO<sub>2</sub> gas saturations 30 years after the fresh water aquifer was depressurized, using the core-flood relative permeabilities. Vertical exaggeration is 5x.

When the brine first reaches the freshwater, it still contains a relatively large amount of dissolved CO<sub>2</sub> (see Figure 2). This dissolved CO<sub>2</sub>, along with the dissolved salt, causes the brine to be denser than the fresh water, and the fluid tends to flow along the base of the aquifer (Figures 8 and 9).

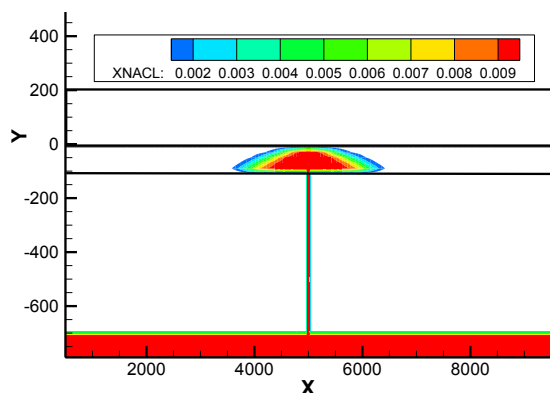


Figure 8. Simulated aqueous salt mass fractions 30 years after the fresh water aquifer was depressurized, using the core flood relative permeabilities.

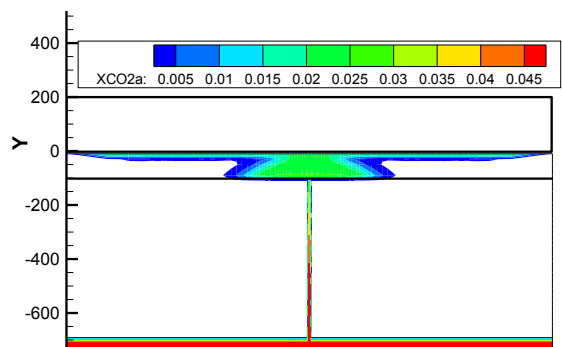


Figure 9. Simulated dissolved CO<sub>2</sub> mass fractions 30 years after the fresh water aquifer was depressurized, using the core flood relative permeabilities.

The mobile gas phase, however, moves upward through the freshwater aquifer, eventually accumulating along the base of the upper confining layer. At 30 years, the CO<sub>2</sub> gas phase extends to the edges of the model, 5000 m away from the fault zone. This accumulated CO<sub>2</sub> could acidify the groundwater, and if the CO<sub>2</sub> plume is intercepted by a shallow well, it could discharge directly to the surface. In the absence of an upper confining layer, the CO<sub>2</sub> gas could easily reach the vadose zone and eventually be discharged at the ground surface.

The simulation was repeated using the exsolution relative permeabilities (Figures 4 and 5). In this case, the extent of the CO<sub>2</sub> gas phase in the drinking water aquifer is much smaller (Figure 10).

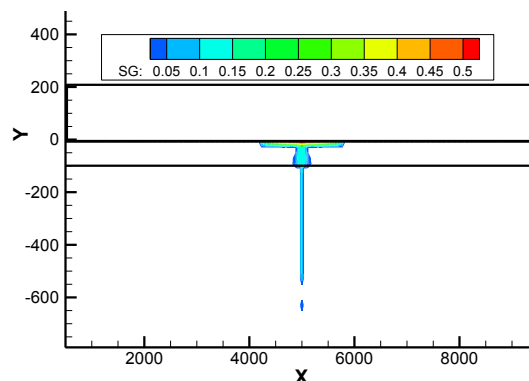


Figure 10. Simulated CO<sub>2</sub> gas saturations 30 years after the fresh water aquifer was depressurized, using the exsolution relative permeabilities.

The smaller extent of the gas phase is due mainly to the lower mobility of the exsolved gas phase. In addition, the aqueous-phase plumes of dissolved salt (Figure 11) and CO<sub>2</sub> (Figure 12) are also substantially smaller in this case. This is due in part to the lower aqueous-phase relative permeability observed during exsolution. It is also due to the accumulation of immobile or low mobility gas phase in the fault zone. These combined effects reduce the brine flow up the fault.

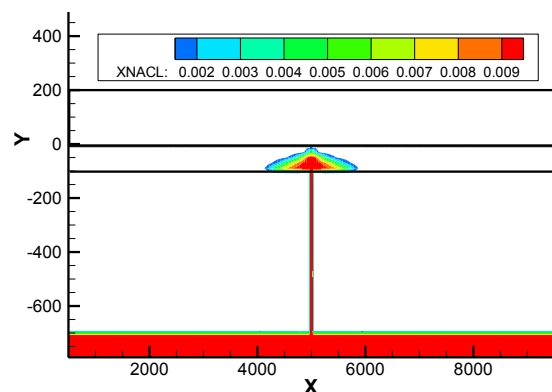


Figure 11. Simulated aqueous phase salt mass fractions 30 years after the fresh water aquifer was depressurized, using the exsolution relative permeabilities.

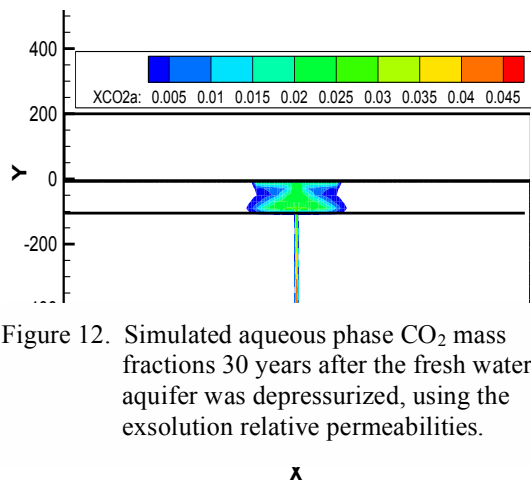


Figure 12. Simulated aqueous phase CO<sub>2</sub> mass fractions 30 years after the fresh water aquifer was depressurized, using the exsolution relative permeabilities.

## SUMMARY

Brine containing dissolved CO<sub>2</sub> can be mobilized upward due to modest hydraulic gradients. As the brine becomes depressurized,

the CO<sub>2</sub> comes out of solution, forming a gas phase (at subcritical pressures). Recent experiments have shown that the relative permeability of the exsolved gas phase is very low. This low relative permeability limits the mobility of the exsolved gas phase compared to a traditional relative permeability function. However, in high permeability systems, the exsolved gas phase may still exhibit some mobility, especially at shallow depths, where the density contrast between the water and gas phases is very large. In this case, the high buoyancy force allows some migration despite the very low gas-phase relative permeability.

## ACKNOWLEDGMENT

This work was supported by the US EPA through STAR Grant #834383.

## REFERENCES

- Bachu, S., W.D. Gunter and E.H. Perkins, 1994, Aquifer disposal of CO<sub>2</sub>: hydrodynamic and mineral trapping, *Energy Conversion and Management*, 35(4), 269-279.
- Benson, S.M. and P. Cook, Coordinating Lead Authors., 2005, "Underground Geological Storage," IPCC Special Report on Carbon Dioxide Capture and Storage, Chapter 5. Intergovernmental Panel on Climate Change, Cambridge University Press, Cambridge, U.K.
- Burton, M. and S. Bryant, Eliminating buoyant migration of sequestered CO<sub>2</sub> through surface dissolution: implementation costs and technical challenges, SPE 110650, Proceedings, 2007 SPE Ann. Tech. Conf. Exhib., Anaheim, CA, 11-14 November, 2007.
- Burton, M. and S.L. Bryant, 2008, Surface dissolution: minimizing groundwater impact and leakage risk simultaneously, presented at the 9<sup>th</sup> International Conference on Greenhouse Gas Control Technologies (GHGT-9), 16-20 November, 2008, Washington, DC.
- Campbell, B., 2008, Development and Application of a Ground-Water Flow and Management Model of the Chesterfield County Region in South Carolina. Clemson

- Hydrogeology Symposium, Clemson University.
- Charbeneau, R., 2007, LNAPL Distribution and Recovery Model (LDRM) Volume 1: Distribuion and Recovery of Petroleum Hydrocarbon Liquids in Porous Media, American Petroleum Institute API Publication 4760.
- Doughty, C., 2007, Modeling geologic storage of carbon dioxide: comparison of non-hysteretic and hysteretic characteristic curves, *Energy Conversion and Management*, 48, 1768-1781.
- Ennis-King, J.P., and L. Paterson, 2005, Role of convective mixing in the long-term storage of carbon dioxide in deep saline formations, *SPE J* 10(3):349-356.
- Falta, R.W., I. Javandel, K. Pruess, and P.A. Witherspoon, 1989, Density-Driven Flow of Gas in the Unsaturated Zone Due to the Evaporation of Volatile Organic Compounds, *Water Resources Research*, Vol. 25, No. 10.
- Farajzadeh, R., H. Salimi, and P.La.H.B. Zitha, 2007, Numerical simulation of density driven natural convection in porous media with applications for CO<sub>2</sub> injection projects, *Int J Heat Mass Transfer* 50(25-26):5054-5064.
- Hassanzadeh, H., M. Pooladi-Darvish, and D.W. Keith, 2007, Scaling behaviour of convective mixing with application to geological storage of CO<sub>2</sub>, *AIChE J* 52:1121-1131.
- Leonenko, Y. and D.W. Keith, 2008, Reservoir engineering to accelerate the dissolution of CO<sub>2</sub> stored in aquifers, *Environ. Sci. Technol.* 42, 2742-2747.
- Lindeberg, E. and D. Wessel-Berg, 1997, Vertical convection in an aquifer column under a gas cap of CO<sub>2</sub>, *Energy Conversion and Management*, 38(Suppl.):S229-S234.
- Mualem, Y., 1984, A modified dependent-domain theory of hysteresis, *Soil Science*, 137:5, 283-291.
- NETL, 2007, Carbon Sequestration Atlas of the United States and Canada, U.S. Department of Energy, National Energy Technology Laboratory. Available from [http://www.netl.doe.gov/technologies/carbon\\_seq/refshelf/atlas/ATLAS.pdf](http://www.netl.doe.gov/technologies/carbon_seq/refshelf/atlas/ATLAS.pdf)
- Nordbotten J.M., D. Kavetski, M.A. Celia, and S. Bachu, 2008, A semi-analytical model estimating leakage associated with CO<sub>2</sub> storage in large-scale multi-layered geological systems with multiple leaky wells, *Environmental Science & Technology*, doi:10.1021/es801135v.
- Pruess, K., 2005a, ECO2N: A TOUGH2 Fluid Property Module for Mixtures of Water, NaCl, and CO<sub>2</sub>, Lawrence Berkeley National Laboratory Report LBNL-57952.
- Pruess, K., 2005b, Numerical Studies of Fluid Leakage from a Geologic Disposal Reservoir for CO<sub>2</sub> Show Self-Limiting Feedback between Fluid Flow and Heat Transfer, *Geophys. Res. Lett.*, Vol. 32, No. 14, L14404, doi:10.1029/2005GL023250, July 2005. (LBNL-57362).
- Pruess, K. and J. Garcia, 2002, Multiphase flow dynamics during CO<sub>2</sub> disposal into saline aquifers, *Environmental Geology*, 42:282-295
- Pruess, K., and N. Spycher, 2007, ECO2N – A fluid property module for the TOUGH2 code for studies of CO<sub>2</sub> storage in saline aquifers, *Energy Conversion and Management*, 48, 1761-1767.
- van Genuchten, M.T., 1980, A closed-form equation for predicting the hydraulic conductivity of unsaturated soils, *Soil Sci. Soc. Am. J.*, 44, 892-898.
- Zuo, L., S. Krevor, R.W. Falta, and S.M. Benson, 2012, An Experimental Study of CO<sub>2</sub> Exsolution and Relative Permeability Measurements during CO<sub>2</sub> Saturated Water Depressurization, *Transport in Porous Media*, Vol. 91, Issue 2, p. 459-478.